Dewetting Modes of Thin Metallic Films: Nucleation of Holes and Spinodal Dewetting

J. Bischof, D. Scherer, S. Herminghaus, and P. Leiderer

Department of Physics, University of Konstanz, P.O. Box 5560 M676, D–78434 Konstanz, Germany
(Received 3 April 1996)

We have studied the dewetting of thin liquid metal films (Au, Cu, Ni) on fused silica substrates which occurs after melting with a Q-switched laser pulse. Optical microscopy, scanning electron microscopy, and scanning near field acoustic microscopy reveal two distinctly different modes of the dewetting process: On one hand, we observe heterogeneous nucleation of "dry" circular patches, which grow in diameter during the melting period. On the other hand, an instability of the liquid film against the growth in amplitude of surface waves with a characteristic wavelength is observed, which we believe is the first observation of spinodal dewetting. In contrast, the final structure of the ruptured film depends on whether nucleation or spinodal dewetting is dominant. [S0031-9007(96)00893-9]

Dewetting of metastable thin films from a solid substrate is currently a topic of great interest [1–4]. This is based not only on the applicational relevance, e.g., in thin film technology. Also from a fundamental point of view there are unsolved questions concerning the interpretation of experimentally observed phenomena with respect to the behavior predicted theoretically. Particularly interesting is the self-organized structure evolution in time and space. Often the basics of dewetting have been studied on *liquid* films because heterogeneous influences, i.e., from grain boundaries or stresses, associated with solid films are not as prominent or must not be considered. From the theoretical considerations, dewetting of a metastable liquid film can develop via two different mechanisms [5]: First, nucleation and growth of holes can take place. This process has already been studied in detail experimentally. Redon *et al.* [4] nucleated holes in thin films of alkanes on silicon wafers at temperatures above the glass transition and studied their growth as a function of the surface tension of the alkanes. In general the growth of the holes leads to accumulation of the material along the perimeter of the holes by building up an elevated rim around them. The second process which can lead to dewetting is based on an instability of the film against thermally activated surface waves. According to theory [5–7], this instability ruptures the film spontaneously and a characteristic wavelength of surface modulations with the minimal rise-time should dominate for a given system. This characteristic wavelength should scale with the square of the liquid film thickness [5]. However, the experiments reported so far do not provide an unambiguous demonstration for this behavior. Polystyrene films dewetting from silicon surfaces were found to develop circular holes whose number density scaled with the film thickness [8]. This was taken as evidence for spinodal dewetting as the process responsible for their formation. However, no direct indication for unstable surface waves was found, which in a spinodal process should precede the breakup of the holes. Guerra *et al.* [9] observed rather ordered wavelike dewetting structures in polystyrene films on a glass substrate.

These authors also suggested spinodal dewetting as the underlying process, although the overall appearance of the observed structures deviated strongly from what one would expect on the basis of numerical simulations [7].

The experiments cited above were all done with polymers and organic fluids, which are frequently used as model systems within the field of dewetting of liquid films. In the present experiments, we study in contrast the dewetting of thin liquid *metallic* films on fused silica substrates. It is known that metallic films, evaporated on glass as a flat film, are in a metastable state and dewet upon annealing in the solid as well as in the liquid state [2,10]. Thus we can check the theoretical predictions concerning the dewetting of a liquid film with a totally different system. Since the viscosity of liquid metals is usually lower and the surface energy is higher than for polymers, dewetting takes place on a much shorter time scale, namely in the nanosecond to microsecond range as shown below.

The metal films used (Au, Cu, Ni) with thicknesses ranging from 25 to 50 nm were thermally evaporated on fused silica substrates (rms roughness <1 nm on the 2 μm scale). In order to improve the adhesion of the films, an intermediate layer of a few monolayers of chromium with a thickness less than 2 nm was additionally evaporated. Melting was achieved by a frequency doubled Q-switched Nd:YAG laser pulse ($\lambda = 532$ nm, FWHM 7 ns) with a beam profile close to TEM$_{00}$. The laser pulse was mildly focused at nearly normal incidence to a spot diameter of about 1 mm. The time-dependent reflectivity $R(t)$ of the films was measured at an angle of incidence of 45° with an s-polarized cw HeNe laser ($\lambda = 632.8$ nm, 8 mW) focused to a $1/e$ diameter smaller than 20 μm in order to determine locally the processes in the film following the irradiation with the laser pulse. The reflected intensity of the probe laser was detected by a *p-i-n* photodiode with a rise time less than 1 ns and registered by a fast oscilloscope. *Ex situ* characterization of the film topography was carried out by optical microscopy, scanning near field acoustic microscopy (SNAM) [11,12], and electron microscopy.

To demonstrate the versatility and usefulness of the information obtained from a reflectivity measurement we show in Fig. 1 the reflectivity $R(t)$ of a 47 nm Au film on a fused silica substrate, irradiated with a laser pulse at an energy density of 320 mJ/cm^2 (which is below the threshold for film rupture by dewetting). The changes in $R(t)$, compared with calculated values for the temperature change of the reflectivity on the basis of temperature dependent optical constants from the literature [13], revealed that the film was molten from $t \approx 5$ ns on. After the irradiation with the laser pulse the metal film cooled down due to heat flow into the substrate. The sudden change in the slope of $R(t)$ at $t = 185$ ns marks the onset of resolidification, which was completed some nanoseconds later due to the very high quench rates (up to 10^{11} K/s) involved. The solidified film thus represents a snapshot of the film structure at the moment of solidification. The melt duration could be directly determined for the used energy density to be $t_m \approx 180$ ns, which is labeled in the graph. Afterwards the film cooled down further and the reflectivity returned on a longer time scale to the original value, indicating that in this case no irreversible changes occurred within the probed area of about 20 μm in diameter. Under an optical microscope, no evidence for film rupture could be found across the whole molten area.

For higher pulse laser energy densities, however, $R(t)$ was found to display large fluctuations connected with irreversible changes. It is important to note that these fluctuations are observed after an incubation time which is long compared to the laser pulse. Optical microscopy afterwards revealed that circular holes had formed in the film. This behavior was observed also for copper and nickel films.

For increasing energy density the holes grew in diameter. Figure 2(a) shows the central part of an irradiated area of a 40 nm thick Cu film taken with an optical microscope in the transmission mode. Isolated holes and

holes which have merged during the growth process are visible as brighter areas. (This confirms that the metal does not wet the glass substrate even in the liquid phase [10].) The latter developed distinct ridges between them which finally became unstable and broke up into droplets via the Rayleigh instability in equivalence to the behavior observed for thin polymer films [3]. The structures are preserved due to the high quench rates associated with the ns-laser pulse heating which lead to solidification within a few tens of nanoseconds. Thus the structures could develop only over a limited period in time—essentially the melt duration—and resolidification preserved them.

Figure 2(b) shows a topographic line scan across a typical hole taken with a SNAM. One finds an outer elevated rim around the hole, whose excess volume within our accuracy corresponds to the material removed from the "dry" patch. This indicates that material is essentially conserved in the film, i.e., evaporation can be neglected. In fact, a rough estimate of the material thermally evaporated during the time where the film is at elevated temperature yields, due to the short time scales involved, only a few monolayers.

Deeper insight into the underlying mechanism can be gained from an analysis of the whole irradiated area. First, the positions of neighboring holes appear to be uncorrelated. Second, the diameter of holes increases from outer regions to the center of the molten area, having a predominant size at a given distance to the center. Here the advantage of the used experimental setup is that, due to the lateral Gaussian profile in the energy density of the laser pulse in our experiment, the scenarios after different melt durations and thus different stages of dewetting are preserved across the spot upon one single laser pulse. Thus the diameter of the holes is somewhat like a "stop-watch" for the local melt duration.

Furthermore, examination with a scanning electron microscope revealed that in the center of many holes there is a small hillock which may have provided the center of nucleation for the holes. This observation suggests that the holes were nucleated heterogeneously. Earlier experiments on pulse laser treatment of a 80 nm thick Cu film on sapphire substrate [10] also indicated that heterogeneous nucleation is responsible for the formation of circular holes. There, also clearly prior to evaporation, formation of holes was found, where the density of holes was correlated to the density of defects on the substrate.

The structures described so far were very similar to the ones observed by Redon et al. [4] upon external nucleation and those interpreted as spinodal dewetting by Reiter [8]. That spinodal dewetting results in strongly different structures (at least in our systems) will be presented in the next paragraphs and can be summarized as follows: In addition to the described nucleation we directly observe a second distinguishable mechanism of dewetting, namely the growth of surface modulations, which is theoretically predicted for a nonwetting fluid [5]. To minimize the influence of possible surface contamination like oxide
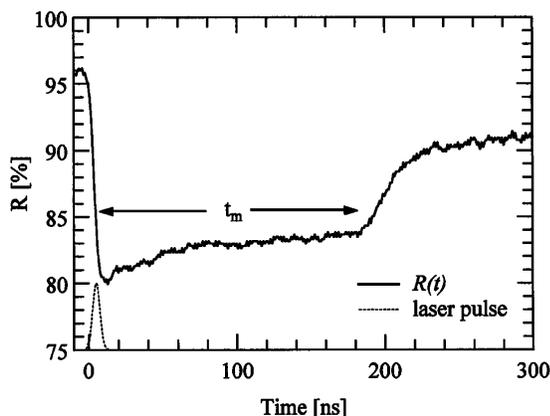
FIG. 1. Time-resolved reflectivity of the HeNe probe laser for a sample consisting of 47 nm Au on fused silica upon the influence of the pulse laser with the energy density of 320 mJ/cm^2. The melt duration $t_m \approx 180$ ns and the schematic temporal shape of the laser pulse is indicated in the graph. The laser intensity is below the threshold for dewetting.
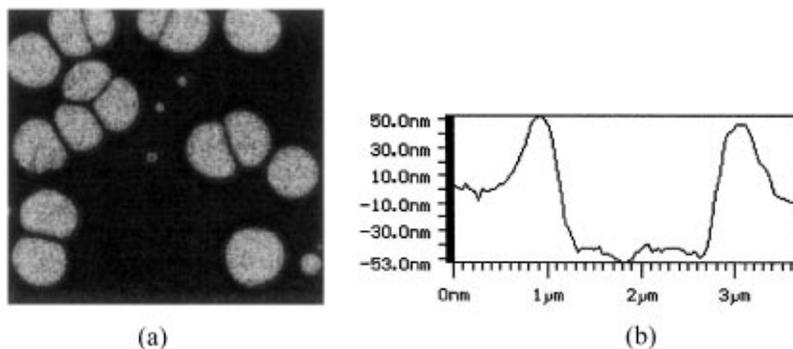
FIG. 2.   (a) Picture taken with an optical microscope in transmission after the laser treatment of a 40 nm thick Cu film on fused silica. (b) Topographic line scan across a typical hole taken with a scanning near field acoustic microscope (SNAM).

layers we focused in this context on investigations of thin Au films. Typical resulting structures can be seen in the two pictures shown in Fig. 3. They were taken with an optical microscope in the reflection mode from the central part of a molten area of a sample with a 47 nm thick Au film. The energy density, and thus the melt duration, increases from the bottom to the top of the pictures due to the spatial profile of the laser pulse.

From Fig. 3(a) it is obvious that two different types of holes dominate the picture. The bigger circular holes with typical diameters of approximately 5 μm correspond to the already described nucleation. Apart from those, also irregularly shaped holes with typical sizes near 2 μm are visible. The latter break through via a height modulation of the surface with a characteristic length scale. This can be seen from Fig. 3(b), which shows the same area as Fig. 3(a) but with the microscope slightly defocused in order to make the surface modulations more prominent.

These surface modulations were also confirmed by SNAM measurements. An example of a topographic line scan is plotted as an inset in Fig. 4. The SNAM measurements reveal that the amplitude of the (nearly sinusoidal) height modulations increase with decreasing distance from the center of the laser pulse spot. Thus the temporal development can be clearly determined: For higher energy density (i.e., longer melt duration) the amplitude of the surface modulations increases, and finally the modulations break through onto the substrate forming holes in the film. The characteristic length scale of the

surface modulations for the example shown in Fig. 3 can be extracted to be 2.4 ± 0.4 μm. It is remarkable that the appearance of surface modulations in Fig. 3(b) is very similar to theoretical calculations on spinodal dewetting [7] presented earlier. Further corroboration of the instability of the liquid surface as dewetting mechanism was gained by the measured dependence of the characteristic wavelength on the metal film thickness as shown in Fig. 4. The dashed line corresponds to a quadratic dependence of the characteristic wavelength λ_m on the film thickness, $\lambda_m = 2\pi \sqrt{\frac{2}{3}} \, d^2/\alpha$, as predicted by the theory of spinodal dewetting [5] with the parameter α being characteristic of the material combination substrate/film.

According to this theory, the amplitude of the unstable surface waves grows exponentially in time. For the characteristic wavelength the rise time τ_m is

$$\tau_m = \frac{4}{3} \frac{d^5}{\alpha^4 v} \, , \tag{1}$$

with a velocity v given approximately by the ratio of surface energy γ to viscosity η. Data from the literature ($\gamma = 1.15$ N/m [14], $\eta = 5.38 \times 10^{-3}$ Ns/m^2 [15]) for liquid gold at the melting temperature yield a value of $v = 214$ m/s. From the fit in Fig. 4 we can extract the constant α to be 4.3 ± 1.4 nm. In liquids whose cohesion is solely due to van der Waals forces, this quantity is only about an interatomic spacing [5]. However, in metals (with free electrons) this may be strongly different. Furthermore, the surface tension of the gold may be
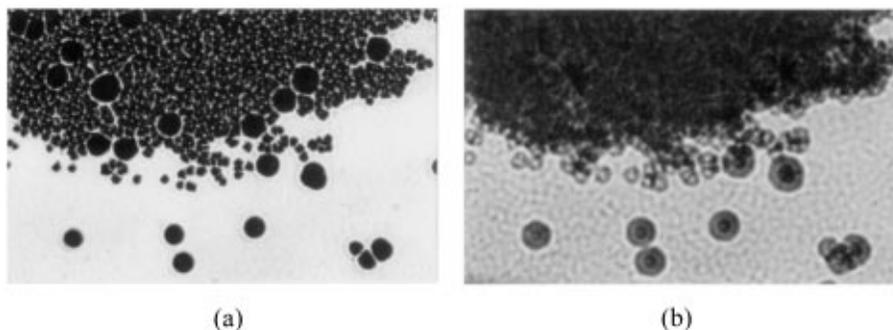

FIG. 3.   Pictures taken with an optical microscope in reflection of the central part of a molten area. The sample consisted of a 47 nm thick Au film on fused silica. Both pictures display the same area. The only difference is that in picture (b) the film surface is slightly out of focus, thus enhancing the contrast due to modulations of the film surface in the regions without holes.
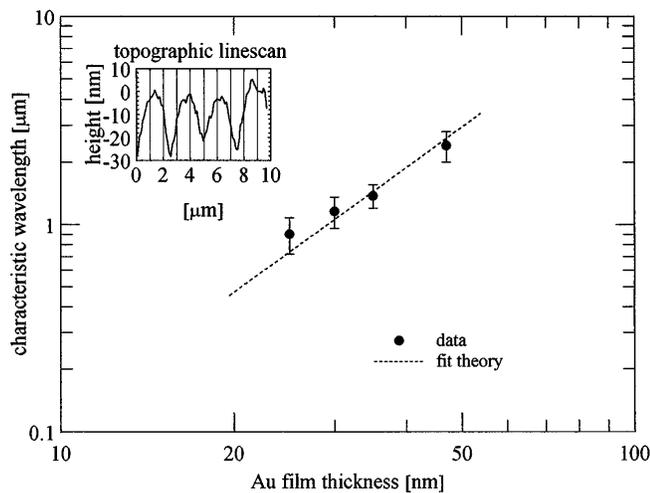
FIG. 4. Dependence of the characteristic wavelength of the surface modulations on Au film thickness. The fit is based on the dependence predicted by the theory of spinodal dewetting. The inset shows a topographic linescan of the surface modulations at a 47 nm thick Au film, as it can be extracted from the SNAM measurements.

drastically reduced by alloying with the Cr adhesion layer [15], which would also give rise to an enlarged α. With $\alpha = 4.3$ nm Eq. (1) yields the time scale on which these structures are expected to develop according to the dewetting theory. The calculated values of τ_m range from about 180 ns for the thinnest (25 nm) up to a 4200 ns for the thickest (47 nm) investigated film. The typical melt durations, which are the periods in time where the structures can develop, are in fair agreement with these calculated values. We take this consistency of the observed lateral evolution of the structures with the temporal evolution as a clear indication that we have, for the first time unambiguously, observed spinodal dewetting of thin liquid films.

Analogous experiments have been performed with chemical vapor deposited–evaporated Si films of 80 nm thickness on fused silica. With those we have obtained periodic surface modulations very similar to the ones described above. Since there was no adhesive layer necessary with the silicon films, this demonstrates that the observed effects are not connected to the presence of the chromium layer. In principle one might argue that plasma formation or stimulated scattering of the pulsed laser light from surface waves [16] could be responsible for the observed structures. Plasma formation can be excluded because it takes place at distinctively higher energy densities than those applied here. The formation of the structures by scattering of the pulsed laser light from surface waves can be excluded by the following argument.

As already mentioned the energy density increased towards the top of Fig. 3(a), thus in the upper part of the picture dewetting has evolved further. Additionally, we know that the circular holes have developed after an incubation time being long compared to the pulse duration. If the surface modulations (and the hillocks) were formed by a pulse laser-induced process, the bigger holes developing

later on could never be so nicely circular. If there were preexisting surface modulations or even hillocks, only irregularly shaped holes could grow (if they could develop at all). Thus the only possible mechanism is that the rupture by surface modulations occurred after the nucleation on a time scale comparable to the growth of the circular holes. Consequently, the surface modulation amplitude increased with increasing melt duration, and after some time broke through onto the substrate forming in an early stage the irregularly shaped holes and finally developed to the hillocks as observed in the top of Fig. 3(a).

In conclusion, we have observed two coexisting mechanisms of dewetting: on one hand, nucleation of circular holes and, on the other hand, an instability of the film against surface waves. The nucleation of holes is apparently based on a heterogeneous process starting surface inhomogeneities. Concerning the spinodal dewetting, a behavior in agreement with earlier theoretical predictions was for the first time observed and clearly identified. In contrast to what is widely believed the resulting structures are different for the two dewetting mechanisms.

[1] For a review on wetting, see, for example, M. Schick, in *Liquids at Interfaces,* Proceedings of the Les Houches Summer School, Session XLVIII, edited by J. Charvolin *et al.* (Elsevier, Amsterdam, 1990).

[2] D. J. Srolovitz and M. G. Goldiner, J. Met. **3**, 31 (1995).

[3] G. Reiter, Langmuir **9**, 1344 (1993).

[4] C. Redon, F. Brochard-Wyart, and F. Rondelez, Phys. Rev. Lett. **66**, 6 (1991); **66**, 715 (1991).

[5] F. Brochard Wyart and J. Daillant, Can. J. Phys. **68**, 1084 (1990).

[6] E. Ruckenstein and R. K. Jain, Faraday Trans. **70**, 2 (1974); **70**, 132 (1974).

[7] A. Vrij, Discuss. Faraday Soc. **42**, 23 (1966).

[8] G. Reiter, Phys. Rev. Lett. **68**, 1 (1992); **68**, 75 (1992).

[9] J. M. Guerra, M. Srinivasarao, and R. S. Stein, Science **262**, 1395 (1993).

[10] M. J. Godbole, A. J. Pedraza, D. H. Lowndes, and J. R. Thompson, Mater. Res. Soc. Symp. Proc. **235**, 583 (1992).

[11] P. Günther, U. Ch. Fischer, and K. Dransfeld, Appl. Phys. B **48**, 89 (1989).

[12] P. Güthner, E. Schreck, K. Dransfeld, and U. Ch. Fischer, in *Scanning Tunneling Microscopy and Related Materials,* edited by R. J. Behm *et al.* (Kluwer Academic Publishers, Dordrecht, The Netherlands, 1990), p. 507.

[13] M. Otter, Z. Phys. **161**, 539 (1961).

[14] I. Egry, G. Lohoefer, and G. Jacobs, Phys. Rev. Lett. **75**, 4043 (1995).

[15] T. Iida and R. I. L. Guthrie, *The Physical Properties of Liquid Metals* (Oxford University Press, Oxford, 1987).

[16] A. M. Prokhorov, V. I. Konov, I. Ursu, and I. N. Mihailescu, *Laser Heating of Metals* (Adam Hilger, New York, 1990), Chap. 5.